NUMERICAL SIMULATION OF DIFFUSION OF MULTIPLE METAL VAPOURS IN A TIG ARC PLASMA FOR WELDING OF STAINLESS STEEL


K. Yamamoto


M. Tanaka


S. Tashiro


K. Nakata


E. Yamamoto


K. Yamazaki


K. Suzuki

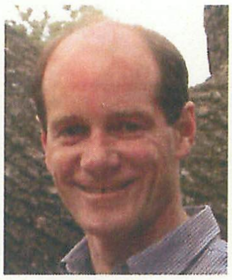
A.B. Murphy

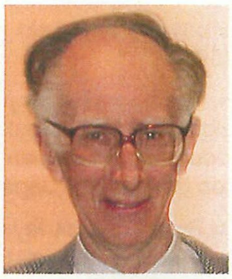
J.J. Lowke

ABSTRACT

In the present paper, a TIG arc in helium or argon is modelled, taking into account the contamination of the plasma by the metal vapour from a stainless steel weld pool. Iron, chromium and manganese are considered the metal vapour species in this model. A viscosity approximation is used to express the diffusion coefficient in terms of the viscosities of the shielding gas and the metal vapour. The time-dependent, two-dimensional distributions of temperature, velocity and metal vapour concentrations of iron, chromium and manganese are predicted, together with the weld penetration, as a function of time for a 150 A arc at atmospheric pressure, for both helium and argon welding gases. The distribution of the metal vapours depends on the diffusion term and the convection term. Due to the cathode jet, the convection term has a strong effect. Consequently, it is found that the metal vapours expand in the radial direction and are concentrated around the weld pool surface. The concentration of manganese vapour is larger than those of iron and chromium vapours, despite the fact that the proportion of manganese in stainless steel is significantly smaller.

IIW-Thesaurus keywords: *Reference lists; Simulating; Stainless steels; Steels; Welding.*

Mr. Kentaro YAMAMOTO (k-yama@jwri.osaka-u.ac.jp), Prof. Manabu TANAKA (tanaka@jwri.osaka-u.ac.jp), Dr. Shinichi TASHIRO, Prof. Kazuhiro NAKATA are with Joining and Welding Research Institute, Osaka University, Osaka (Japan). Mrs. Eri YAMAMOTO, Mr. Kei YAMAZAKI and Mr. Keiichi SUZUKI are with the Welding Company, Kobe Steel, Ltd., Kanagawa (Japan). Dr. Anthony B. MURPHY and Dr. John J. LOWKE are with CSIRO Materials Science and Engineering, Sydney (Australia).

Doc. IIW-1963-08 (ex-doc. SG-212-1121r1-08) recommended for publication by SG-212 "The physics of welding".

1 INTRODUCTION

During the arc welding process, four states of matter, solid, liquid, gas and plasma, simultaneously exist and interact within a volume of only 1 cm^3. The temperature range is wide, ranging from about 20 000 K in the arc plasma, about 3 000 K in the tungsten cathode, about 2 000 K in the molten steel, down to room temperature in the surrounding regions [1]. Due to the remarkable progress in computer simulation and observation techniques recently, it has become possible to understand the phenomena in arc welding processes quantitatively [2, 3]. However, it has not been possible to accurately predict the welding parameters, such as the arc voltage and the weld geometry. It is known empirically that the arc voltage in a TIG arc on water-cooled copper differs from that in a TIG arc during welding. This phenomenon is caused by the metal vapour from the weld pool surface. For a full understanding and accurate prediction of these parameters, it is necessary to understand the behaviour of metal vapour in the arc plasma.

Metal atoms generally have more low energy, excited states and are more easily ionized, than atoms of shielding gases such as argon and helium. These characteristics contribute to an increase of the radiative emission coefficient and the electric conductivity of the plasma. It is estimated that the former affects the thermal pinch effect and the energy transfer efficiency from the arc to the workpiece and that the latter affects the current density distribution. Tashiro *et al.* [4] conducted a virtual experiment by numerically simulating a pure helium arc, as well as an arc in helium uniformly mixed with 30 mol % iron atoms, which showed that an obvious arc constriction occurred for the latter case. Furthermore, they reported that the energy efficiency greatly decreased from about 80 % to about 35 %. These results suggested that the existence of metal vapour changed the heat source property in the arc welding process, consequently changing the size and shape of the molten pool.

As noted above, there have been significant advances in the simulation of arc welding. For example, a numerical simulation of gas metal arc welding, including the formation of droplets from a steel wire electrode, has been reported [5]. However, the welding gas was pure argon and the effect of metal vapour was not considered. On the other hand, calculations of the behaviour of metal vapour in an atmospheric pressure plasma have also been reported [6]. But the conditions were far from those of welding because a solid electrode with a constant temperature was assumed. It is important for accurate understanding of the arc welding process to consider the mixing of the metal vapour in a model that takes into account the tungsten cathode, the arc plasma and the weld pool.

The authors developed a numerical model of stationary TIG arc welding, taking into account the metal vapour produced from the weld pool surface [7]. The anode was assumed to be a stainless steel. In practice, metal vapour species in an arc plasma with a stainless steel anode include Fe, Cr, Ni, Mn and so on [8]. However, only iron vapour was considered in the model.

In the present paper, we use a numerical model of stationary TIG arc welding, taking into account the iron, chromium and manganese vapours produced from the weld pool surface. We also simulate the distribution of the metal vapours, the plasma temperature, fluid flow velocity and the formation of the weld pool.

2 SIMULATION MODEL

The tungsten cathode, arc plasma and anode are described relative to cylindrical coordinates, assuming rotational symmetry around the arc axis. The calculation domain is shown in Figure 1. The diameter of the tungsten cathode is 3.2 mm with a 60-degree conical tip. The anode is of stainless steel,the composition of which is given in Table 1 for the present model. Helium shielding gas is introduced from the outside of the cathode on the upper boundary at the flow rate of 30 l/min.

The convection in the weld pool is influenced by the shear stress due to the convective flow of the cathode jet, the Marangoni force due to the gradient in the surface tension of the weld pool, buoyancy due to gravity

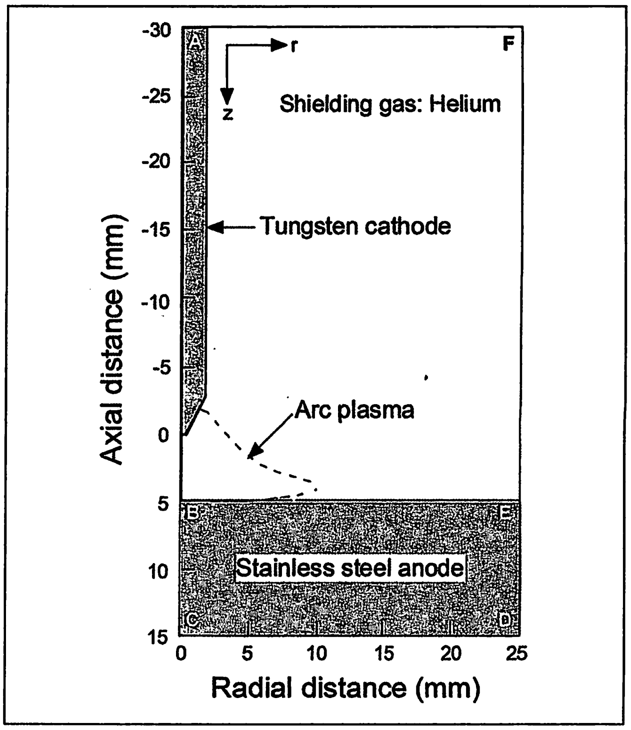

Figure 1 – Schematic illustration of simulation domain

Table 1 – Composition of the stainless steel used in the model

Iron	Chromium	Manganese
80.5 wt %	18 wt %	1.5 wt %

and the electromagnetic pinch force due to the arc current. Only the driving forces of the weld pool convection at the boundary between the weld pool and the arc plasma are explained here. First, the shear stress is already included in radial momentum conservation through the viscosity at the anode surface. Second, the Marangoni force is given by [9]

$$M_A = \frac{\partial}{\partial z}\left(\frac{\partial \gamma}{\partial T}\frac{\partial T}{\partial r}\right) \qquad (1)$$

where

T is temperature,
γ is the surface tension of the weld pool.

In this paper, stainless steel is assumed to have low sulphur content (about 10 ppm) and the variation of the surface tension at the weld pool surface is assumed to decrease linearly with increasing temperature ($\partial\gamma / \partial T = -0.46$ mN/mK) [9].

A species conservation equation expressed by Equation (2) is applied, to take into account the behaviour of the metal vapours [6]. Iron, chromium and manganese vapours are considered in this model. However, to simplify the model and facilitate calculation, those vapours are not calculated simultaneously but are calculated separately, as a He-Fe, He-Cr and He-Mn system.

$$\frac{\partial}{\partial t}(\rho C_i) + \frac{1}{r}\frac{\partial}{\partial r}(r\rho v_r C_i) + \frac{\partial}{\partial z}(\rho v_z C_i) = \frac{1}{r}\frac{\partial}{\partial r}\left(r\rho D_i\frac{\partial C_i}{\partial r}\right) + \frac{\partial}{\partial z}\left(\rho D_i\frac{\partial C_i}{\partial z}\right) \qquad (2)$$

where

t is time,
v_r and v_z are the radial and axial velocities,
ρ is the density,
C_i is mass fraction concentration of metal vapour and
D_i is the binary diffusion coefficient, which is expressed by the viscosity approximation equation:

$$D_i = \frac{2\sqrt{2}(1/M_i + 1/M_g)^{0.5}}{\left[(\rho_i^2/\beta_i^2\eta_i^2 M_i)^{0.25} + (\rho_g^2/\beta_g^2\eta_g^2 M_g)^{0.25}\right]^2} \qquad (3)$$

where

M_i and M_g are the molecular weights of metals and the shielding gas respectively.

Similarly, ρ_i, ρ_g, η_i, η_g are respectively, the density and viscosity of metals and the shielding gas.

β_i, β_g are the constants without dimension, defined as $\beta_i = (D_{ii}\rho_i)/\eta_i$ and theoretically range from 1.2 to 1.543 for various species of gas, such as Ar, He, H_2, N_2, O_2, CO_2 and so on.

It is assumed that $\beta_i = \beta_g = 1.385$, which is based on the mean value of experimental data [10]. The viscosity approximation is not strictly justified, since it does not take into account ionized species and is at best, reasonably accurate [11]; however, it is considered to be a useful first approximation for the arc welding model.

C_i is set to be zero in the cathode area and in the solid area of the anode. However, at the anode surface where the temperature is above the melting point, C_i is set to [6]:

$$C_i = \frac{n_i p_{v,i} M_i}{n_i p_{v,i} M_i + (p_{atm} - n_i p_{v,i})M_g} \qquad (4)$$

where

p_{atm} is atmospheric pressure and
$p_{v,i}$ is the partial pressure of metal vapour, which is a function of the weld pool temperature [12] and
n_i is the mole fraction of a metal in stainless steel.

According to Equation (4), C_i has values between zero and 1.0. For other boundary conditions, $C_i = 0$ at AF and FE shown in Figure 1, and $(\partial C_i / \partial r) = 0$ at the arc axis (AB).

In the present model, plasma properties are dependent on not only the temperature, but also on the mole fraction of iron, chromium and manganese vapours. However, iron, chromium and manganese vapours are all considered as iron vapour in calculating plasma properties for the simplification. Plasma properties at intermediate concentrations of iron vapour are calculated using a linear approximation, based on the properties at 0 mol %, 1 mol %, 10 mol % and 20 mol % [13]. The properties were calculated by assuming the arc plasma to be in the local thermodynamic equilibrium (LTE) and using the Chapman-Enskog approximation [13]. For example, the electrical conductivities, which are significantly affected, are shown in Figure 2. The electrical conductivities are greatly increased by the addition of iron vapour at temperatures below 15 000 K, while the values for mixing ratios, 1 %, 10 % and 20 %, are almost the same.

The other approximations, governing equations and boundary conditions, are given in detail in our previous

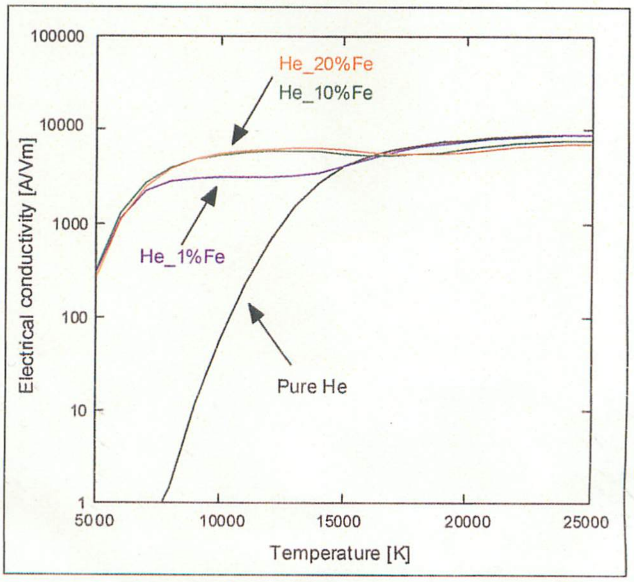

Figure 2 – Dependence of electrical conductivities of helium gas on temperature for each mixing ratio

papers [4, 14]. The governing and auxiliary equations are solved iteratively by the SIMPLEC numerical procedure.

3 CALCULATION RESULTS

The present model is applied to the case of stationary helium TIG arc welding of stainless steel. Figure 3 shows the two-dimensional distribution of temperature and fluid flow velocity at a time 20 s after arc ignition, namely, when the weld pool has grown to a reasonable extent. Figure 4 shows the distributions of iron, chromium and manganese vapours in arc plasma. The distributions of metal vapours depend on the diffusion term and the convection term, as described in Equation (2). Due to the cathode jet, which leads to flow velocities of over 300 m/s in the welding arc, the convection term has a strong effect. Therefore, it is found that distribution of iron vapour expands in a radial direction and is concentrated around the weld pool surface.

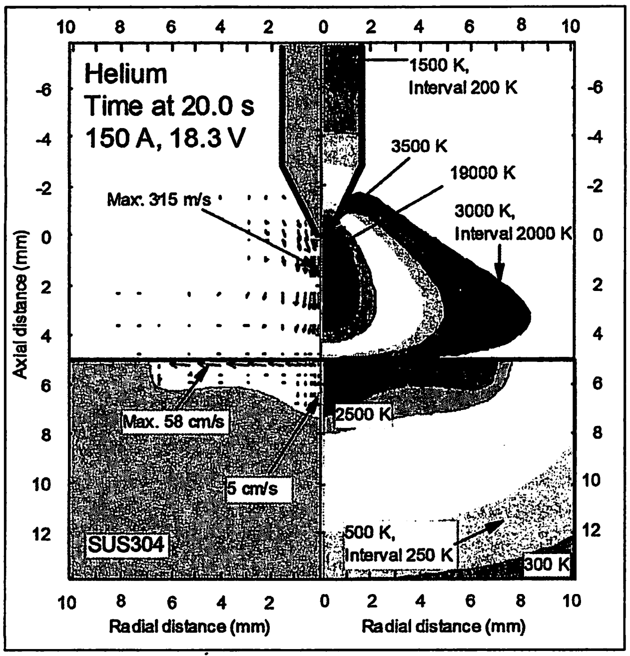

Figure 3 – Calculation result of helium GTA welding for a 150 A, 20 s after arc ignition

Figure 5 shows the radial distribution of metal vapours around the anode surface. The concentrations of iron and chromium vapours are almost the same and the maximum concentrations are about 4 mol %. The maximum concentration of manganese vapour is about 5 mol %. Due to the higher partial pressure of manganese vapour, especially at a low temperature, the concentration of manganese vapour is larger than those of iron and chromium vapours, despite the fact that the proportion of manganese in stainless steel is significantly smaller.

4 CONCLUSIONS

(1) A numerical model for a stationary helium TIG arc welding, taking into account the iron, chromium and manganese vapours produced from the weld pool surface, was used to simulate the distribution of the metal vapours, plasma temperature, fluid flow velocity and the formation of the weld pool.

(2) Due to the cathode jet velocity of over 300 m/s in the welding arc, the convection term strongly affects the

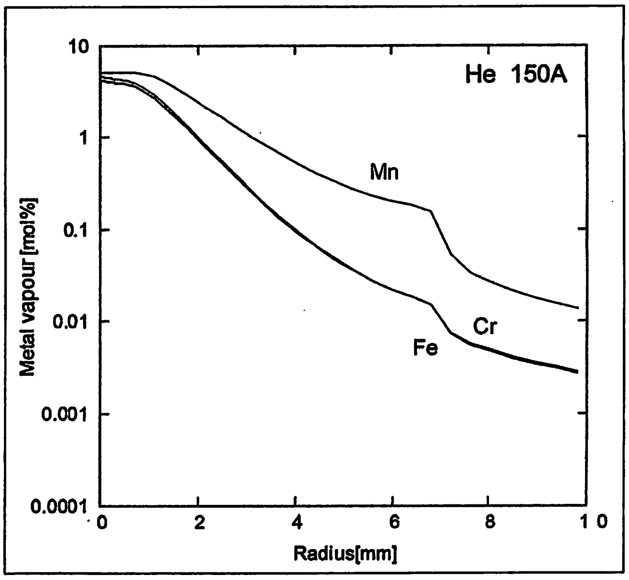

Figure 5 – The radial distribution of metal vapours around the anode surface

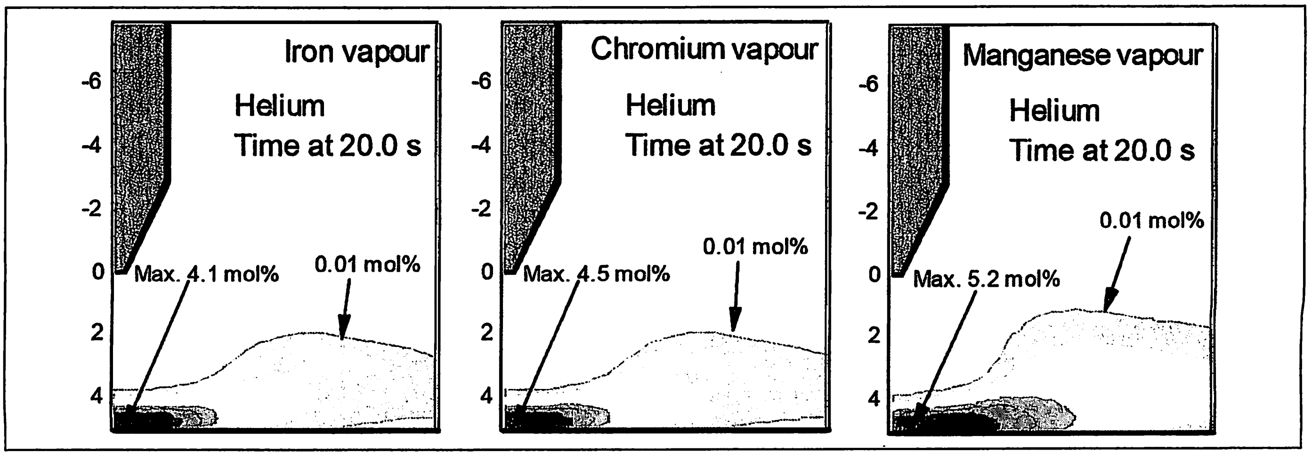

Figure 4 – Distribution of iron, chromium and manganese vapours in arc plasma

distribution of metal vapours. It was found that metal vapours expanded mainly in the radial direction and remained concentrated around the weld pool surface.

(3) The concentration of manganese vapour is larger than those of iron and chromium vapours, despite the fact that the proportion of manganese in stainless steel is significantly smaller.

REFERENCES

[1] Tanaka M., Watanabe T., Isa T., Nishiwaki H.: New development of welding and thermal spraying, Journal of Plasma and Fusion Research, 2006, vol. 82, no. 8, pp. 492-496 (in Japanese).

[2] Fan H.G., Kovacevic R.: The front line of modeling heat and mass transfer in arc welding processes, Journal of the Japan Welding Society, 2007 vol. 76, no. 2, pp. 82-89.

[3] Nishiyama H., Sawada T., Takana H., Tanaka M., Ushio M.: Computational simulation of arc melting process with complex interactions, ISIJ International, 2006, vol. 46, no. 5, pp. 705-711.

[4] Tashiro S., Tanaka M., Nakata K., Iwao T., Koshiishi F., Suzuki K., Yamazaki K.: Plasma properties of helium gas tungsten arc with metal vapor, Quaterly Journal of the Japan Welding Society, 2006, vol. 24, no. 2, pp. 143-148 (in Japanese).

[5] Fan H.G., Kovacevic R.: A unified model of transport phenomena in gas metal arc welding including electrode, arc plasma and molten pool, Journal of Physics D: Applied Physics, 2004, vol. 37, pp. 2531-2544.

[6] Menart J., Lin L.: Numerical study of a free-burning argon arc with copper contamination from the anode, Plasma Chemistry and Plasma Processing, 1999, vol. 19, no. 2, pp. 153-170.

[7] Yamamoto K., Tanaka M., Tashiro S., Nakata K., Yamazaki K., Yamamoto E., Suzuki K., Murphy A.B.: Metal vapor behavior in thermal plasma of gas tungsten arcs during welding, Quarterly Journal of the Japan Welding Society, 2007, vol. 25, no. 3, pp. 443-449 (in Japanese).

[8] Terasaki H., Tanaka M., Ushio M.: Effects of metal vapor on plasma state in helium gas tungsten arcs, Quarterly Journal of the Japan Welding Society, 2002, vol. 20, no. 2, pp. 201-206.

[9] Tanaka M., Lowke J.J.: Predictions of weld pool profiles using plasma physics, Journal of Physics D: Applied Physics, 2007, vol. 40, pp. R1-R23.

[10] Wilke C.R.: A viscosity equation for gas mixtures, Journal of Chemical Physics, 1950, vol. 18, no. 4, pp. 517-519.

[11] Murphy A.B.: A comparison of treatments of diffusion in thermal plasmas, Journal of Physics D: Applied Physics, 1996, vol. 29, pp. 1922-1932.

[12] The Japan Institute of Metals: Edition No. 3 Data Book of Metals, MARUZEN CO., LTD, 1993, pp. 86-92 (in Japanese).

[13] Murphy A.B.: Transport Coefficients of Air, Argon-Air, Nitrogen-Air, and Oxygen-Air Plasmas, Plasma Chemistry and Plasma Processing, 1995, vol. 15, no. 2, pp. 279-307.

[14] Tashiro S., Tanaka M., Nakatani M., Furubayashi M., Yamazaki Y.: Properties of mass and heat transfer for tube cathode arcs, Quarterly Journal of the Japan Welding Society, 2007, vol. 25, no. 1, pp. 3-9 (in Japanese).